NEUROSCIENCE

Impact of parallel fiber to Purkinje cell long-term depression is unmasked in absence of inhibitory input

Henk-Jan Boele[1]*, Saša Peter[1]*, Michiel M. Ten Brinke[1]*, Lucas Verdonschot[1], Anna C. H. IJpelaar[1], Dimitris Rizopoulos[2], Zhenyu Gao[1], Sebastiaan K. E. Koekkoek[1], Chris I. De Zeeuw[1,3]†

Pavlovian eyeblink conditioning has been used extensively to study the neural mechanisms underlying associative and motor learning. During this simple learning task, memory formation takes place at Purkinje cells in defined areas of the cerebellar cortex, which acquire a strong temporary suppression of their activity during conditioning. Yet, it is unknown which neuronal plasticity mechanisms mediate this suppression. Two potential mechanisms include long-term depression of parallel fiber to Purkinje cell synapses and feed-forward inhibition by molecular layer interneurons. We show, using a triple transgenic approach, that only concurrent disruption of both these suppression mechanisms can severely impair conditioning, highlighting that both processes can compensate for each other's deficits.

INTRODUCTION

During eyeblink conditioning, subjects typically hear a short beep or see a light [conditional stimulus (CS)] followed several hundred milliseconds later by an air puff on the eye [unconditional stimulus (US)]. As a result of repeated CS-US pairings, subjects will eventually learn to close their eye in response to the CS, which is called the conditioned response (CR). The CR is not simply a static reflex, but instead an acquired, precisely timed eyelid movement, the kinetic profile of which depends on the temporal interval between the CS and the US (Fig. 1A) [for review, see (*1*, *2*)]. During Pavlovian eyeblink conditioning, memory formation takes place in Purkinje cells (PCs) of defined areas of the cerebellar cortex (*3*–*8*). These PCs receive inputs from the mossy fiber–parallel fiber (PF) system, which conveys sensory CS signals and input from single climbing fibers (CFs), which transmit the instructive US signal (Fig. 1B). During the conditioning process, these PCs acquire a well-timed suppression of their simple spike firing in response to the CS (*6*, *9*, *10*), thereby temporarily disinhibiting the cerebellar nuclei, which drive the overt eyeblink CR.

How can PCs time their simple spike suppression with such millisecond precision? Most models on eyeblink conditioning assume a critical role for long-term depression (LTD) of the PF-PC synapse (*11*, *12*). However, PCs show high firing frequencies that are intrinsically generated, even when the PF input is silenced (*13*–*15*), and animal models lacking PF-PC LTD can have completely normal eyeblink conditioning (*16*, *17*). A second contribution, which, in principle, may actively suppress the intrinsic PC simple spike activity, could be provided by molecular layer interneurons (MLIs), since they provide the PC with a powerful feed-forward inhibition (FFI) (*5*, *18*). However, removal of MLI-PC FFI induces compensation at the PF-PC synapse (*19*) and only mildly impairs eyeblink conditioning (*6*, *20*).

Here, we asked this question: To what extent does a concurrent disruption of PF-PC LTD and MLI-PC FFI affect Pavlovian eyeblink conditioning? To this end, we developed a mouse line in which we aimed to block both synaptic processes simultaneously (Fig. 1C). We generated *GluR2Δ7-L7-Δγ2* mice by crossing *GluR2Δ7* knock-in (KI) mice with *L7-Δγ2* knockout (KO) mice. *GluR2Δ7* KI mice have impaired PF-PC LTD, because they lack the last seven amino acids at the intracellular C-terminal tail, which hampers the interaction of GluR2 with PICK1 (protein interacting with C kinase 1) and GRIP1/2 (glutamate receptor interacting protein 1 and 2), and thereby the internalization of the AMPA receptor (*21*). *L7-Δγ2* KO mice have impaired MLI-PC FFI, as they have a PC-specific ablation of the γ2 subunit of γ-aminobutyric acid type A ($GABA_A$) receptors (Fig. 1C), (*6*, *19*).

RESULTS

We first established in vitro that *GluR2Δ7-L7-Δγ2* mice lack both PF-PC LTD and MLI-PC FFI. For PF-PC LTD induction, we used 100-Hz PF stimulation in conjunction with a single CF stimulation (Fig. 1D) (*22*) at an interstimulus interval of 110 ms, which is an interval that closely mimics those used during eyeblink conditioning (*23*, *24*). We were unable to induce postsynaptic PF-PC LTD in *GluR2Δ7-L7-Δγ2* mice, just like in the *GluR2Δ7* mice [Fig. 1E and table S1; see also (*17*)], whereas LTD could be readily induced in controls and *L7-Δγ2* mice [Fig. 1E and table S1; see also (*19*)]. We found that our LTD protocol briefly induced an initial LTD-like pattern (~2 min after LTD induction) in *GluR2Δ7-L7-Δγ2* mice (Fig. 1D), which is in line with Piochon *et al.* (*22*); they show the same phenomenon using this protocol in patDp/+ mice with similar PF-PC LTD impairments. Most probably, this is due to the high-frequency (100 Hz) PF stimulation. There were no signs of presynaptic neurotransmitter release abnormalities at the PF-PC synapse in *GluR2Δ7-L7-Δγ2* mice, in that paired-pulse facilitation was unaffected following PF stimulation at intervals varying from 50 to 200 ms (Fig. 1F and table S1). To evaluate the inhibitory MLI to PC input, we measured the spontaneous inhibitory postsynaptic currents (sIPSCs) of PCs. We found that these sIPSCs were virtually absent in *GluR2Δ7-L7-Δγ2* mice (Fig. 1G and table S1), similar to what has been reported for *L7-Δγ2* mice (*19*). Thus, *GluR2Δ7-L7-Δγ2* mice show both impaired PF-PC LTD and MLI-PC FFI.

Next, we evaluated performance in eyeblink conditioning. The *GluR2Δ7-L7-Δγ2*, *GluR2Δ7*, *L7-Δγ2*, and control mice all showed a

[1]Department of Neuroscience, Erasmus MC, Rotterdam, Netherlands. [2]Department of Biostatistics, Erasmus MC, Rotterdam, Netherlands. [3]Netherlands Institute for Neuroscience, Royal Academy of Arts and Sciences (KNAW), Amsterdam, Netherlands.
*These authors contributed equally to this work.
†Corresponding author. Email: c.dezeeuw@erasmusmc.nl

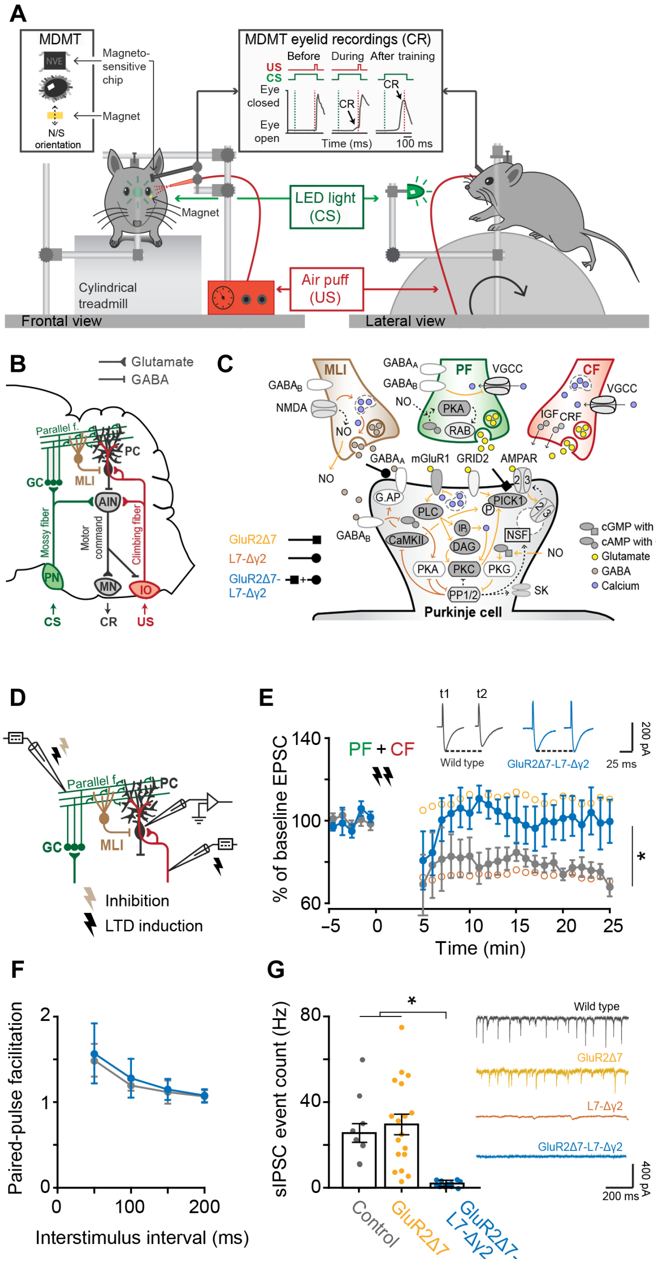

Fig. 1. Eyeblink conditioning setup and confirmation that *GluR2Δ7-L7-Δγ2* mice lack both PF-PC LTD and MLI-PC FFI. (**A**) Mice were placed in a light- and sound-isolating chamber on a freely moving foam treadmill with their head fixed at a horizontal bar. The US consisted of a weak air puff, and the CS was a green light-emitting diode (LED) light. Eyelid movements were recorded with the magnetic distance measurement technique (MDMT). In vivo PC recordings were performed on the same treadmill system. (**B**) Neural circuits essential and sufficient for eyeblink conditioning, explained in detail in the main text. AIN, anterior interposed nucleus; GC, granule cells; IO, inferior olive; MLI, molecular layer interneurons; MN, motoneurons (N. III, VI, and VII); PC, Purkinje cell; PN, pontine nuclei. (**C**) Overview of the main known molecular mechanisms underlying PC plasticity. PF-PC LTD cascades are indicated with ocher arrows, MLI-PC cascades are indicated with brown arrows, and PF-PC long-term potentiation (LTP) and intrinsic plasticity are indicated with dashed arrows. *GluR2Δ7* mice lack PF-PC LTD, *L7-Δγ2* mice lack MLI-PC inhibition, and *GluR2Δ7-L7-Δγ2* mice have disrupted both PF-PC LTD and MLI-PC inhibition. (**D**) Schematic overview of MLI-PC inhibition and PF-PC LTD induction experiments. (**E**) In contrast to controls, *GluR2Δ7-L7-Δγ2* mice show no PF-PC LTD using an induction protocol that consisted of a 100-Hz PF stimulation in eight pulses, followed by a 110-ms delay of single CF activation at 1 Hz for 5 min. (**F**) Applying interstimulus intervals varying from 50 to 200 ms evoked similar levels of paired-pulse facilitation, indicating that baseline PF-PC presynaptic mediated neurotransmitter release is unaltered in *GluR2Δ7-L7-Δγ2* mice. (**G**) *GluR2Δ7-L7-Δγ2* mice show significantly less sIPSCs than controls, indicating that they indeed lack MLI-PC inhibition. For PF-PC LTD and sIPSCs, data of *GluR2Δ7* and *L7-Δγ2* mice are used with permission from Schonewille *et al*. (*17*) and Wulff *et al*. (*19*), respectively. AC, adenylyl cyclase; AMPAR, AMPA receptor (GluR2/3); CaMKII, Ca^{2+}/calmodulin-activated kinase II; cAMP, cyclic adenosine monophosphate; cGMP, cyclic guanylate monophosphate; CRF, corticotropin-releasing factor; $GABA_A$, GABA type A receptor; $GABA_B$, GABA type B receptor; G.AP, $GABA_A$R-associated protein; GC, guanylylcyclase; GluRδ2, glutamate receptor δ2 (GRID2); IP_3, inositol trisphosphate; mGluR1, metabotropic glutamate receptor 1; NMDAR, *N*-methyl-D-aspartate receptor; NO, nitric oxide; PKA, cAMP-dependent protein kinase; PKC, protein kinase C; PKG, cGMP-dependent protein kinase; PLC, phospholipase C; PP1, protein phosphatase 1; PP2, protein phosphatase 2 (A+B); RAB; RAS-related protein RAB3A; SK, small conductance Ca^{2+}-activated K^+ channel; VGCC, voltage-gated Ca^{2+} channel. For complete statistics, we refer to table S1; *$P < 0.05$.

significant increase in CR percentage and fraction eyelid closure [FEC, ranging from 0 (fully open) to 1 (fully closed)] over the course of 10 acquisition sessions (Fig. 2, A and B, and table S2). However, compared to the other three groups, *GluR2Δ7-L7-Δγ2* mice showed severely affected acquisition, in terms of both CR percentage and FEC (Fig. 2, A and B, and table S2). Nevertheless, CR timing, that is, latency to CR onset and CR peak time, was comparable to control mice: CRs initially had no preferred peak time in the CS-US interval (session 1), but after 10 days of training, it peaked around the onset of the expected US (session 10) (Fig. 2C). The smaller FEC but normal CR timing was even more obvious in the CS-only trials presented in the probe session (session 11) (Fig. 3 and table S2).

In line with previous findings (*17*), *GluR2Δ7* mice, lacking only PF-PC LTD, showed normal acquisition of eyelid CRs over the course of 10 days of training. Neither the percentage, nor FEC, nor timing of eyeblink CRs showed any abnormalities compared to control litters (Figs. 2 and 3 and table S2). The *L7-Δγ2* mice, which lack MLI-PC inhibition, had a virtually normal acquisition in terms of CR percentage (Fig. 2A and table S2), but their CRs did not reach the amplitude values of control mice at the end of the training (Figs. 2, B and C, and 3, A and C, and table S2). Although the average CR timing in *L7-Δγ2* mice was not significantly different from that in controls (Figs. 2C and 3, A, B, D, and E, and table S2), we found a significantly higher coefficient of variation (CV) for the latency to CR peak, even after correcting for CR amplitude (Fig. 3H and table S2). These data indicate that the timing of the CR peak in *L7-Δγ2* mice is more jittered compared to that in the other three groups, which is mainly due to a right shift of CR peak times (Fig. 3, A and B).

We could not establish any significant difference between the latency to onset and peak time of the unconditioned response (UR) to the US for any of the groups (fig. S3 and table S2). This shows that the performance of the blink response is intact and that the observed learning deficits are not a result of general impairments in eyelid closure. Thus, over the course of 10 training sessions, *GluR2Δ7-L7-Δγ2* mice acquired only few CRs that had relatively small amplitudes.

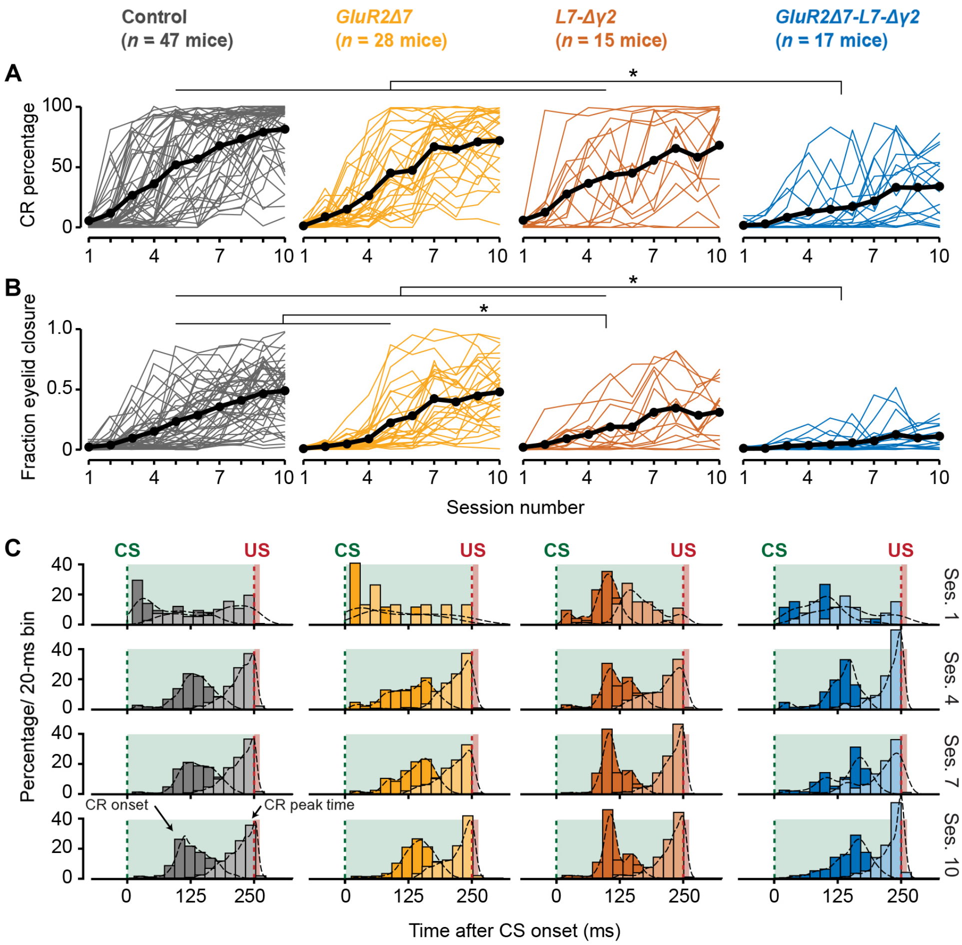

Fig. 2. Acquisition of eyeblink CRs is severely impaired in *GluR2Δ7-L7-Δγ2* mice, whereas *GluR2Δ7* and *L7-Δγ2* mice show normal or only mildly impaired conditioning. (**A** and **B**) Mouse individual (colored) and average (black) learning curves per group showing the development of (A) CR percentage (B) and FECs (or "amplitude of eyelid closure") over the 10 consecutive training sessions. *GluR2Δ7-L7-Δγ2* mice have a significantly slower acquisition and lower CR percentage and FEC than the other three groups. *L7-Δγ2* mice have a mild phenotype with a normal CR percentage but significantly lower FEC at the end of training. No significant difference could be established between controls and *GluR2Δ7* mutants. (**C**) Peristimulus histogram plots with a Gaussian kernel density estimate (black dashed line) showing the distribution of CR onset (dark filled bars) and CR peak time (light filled bars) relative to CS and US onset in paired CS-US trials for sessions 1, 4, 7, and 10. Green dashed lines indicate CS onset, and red dashed lines denote US onset; light green and light red fill indicate CS and US duration, respectively. In all groups, there is a clear development in CR onset and peak time: There are no clearly preferred times in the CS-US interval at the start of training (session 1), but toward the end of training (sessions 7 and 10), CR onset values are centered around 100 to 125 ms after CS onset, and CR peak times are located around the onset of the expected US. In all panels, we refer to "CR" if only trials are included with an FEC > 0.1 and to "FEC" if all trials are included. For complete statistics, we refer to table S2; *$P < 0.05$.

The level of eyeblink conditioning in the *GluR2Δ7-L7-Δγ2* mice was much more affected than what could be expected on the basis of the individual phenotypes observed in the LTD-deficient *GluR2Δ7* mice or the FFI-deficient *L7-Δγ2* mice. These data are in line with our hypothesis that the two mechanisms may both contribute to the simple spike suppression required for eyeblink conditioning (*6*) and that each may compensate for the other's absence to largely preserve conditioned behavior (*25*). Alternatively, the exceptionally strong behavioral phenotype in the *GluR2Δ7-L7-Δγ2* mice could potentially result from general deficits in PC complex spike and simple spike firing levels (*26*), although they appear relatively normal in the *GluR2Δ7* and *L7-Δγ2* mice (*17*, *19*). We therefore recorded PC activity in the anterior lobe of awake *GluR2Δ7-L7-Δγ2* mice, which should have the characteristic firing patterns of zebrin-negative modules, including that of the eyeblink microzone (*5*, *6*, *14*) (Fig. 4A). The complex spike activity of *GluR2Δ7-L7-Δγ2* mice showed an average firing frequency of 1.13 Hz [95% confidence interval (CI), 0.91 to 1.34], and the simple spike pause following the complex spike was, on average, 15.55 ms (95% CI, 14.16 to 16.94), both frequencies being indistinguishable from those of *GluR2Δ7* mice, *L7-Δγ2* mice, or controls (Fig. 4B and table S3). Likewise, their simple spike firing frequencies, which were relatively high at 105.07 Hz (95% CI, 94.55 to 115.59), as expected for the anterior lobe (*14*), were not significantly different from those of the other mutant lines or controls (Fig. 4C and table S3). Moreover, the regularity [that is, coefficient of variation for adjacent intervals (CV2)] of simple spike activity of PCs in the anterior lobe of *GluR2Δ7-L7-Δγ2* mice was not significantly different from that in control mice (Fig. 4D and table S3).

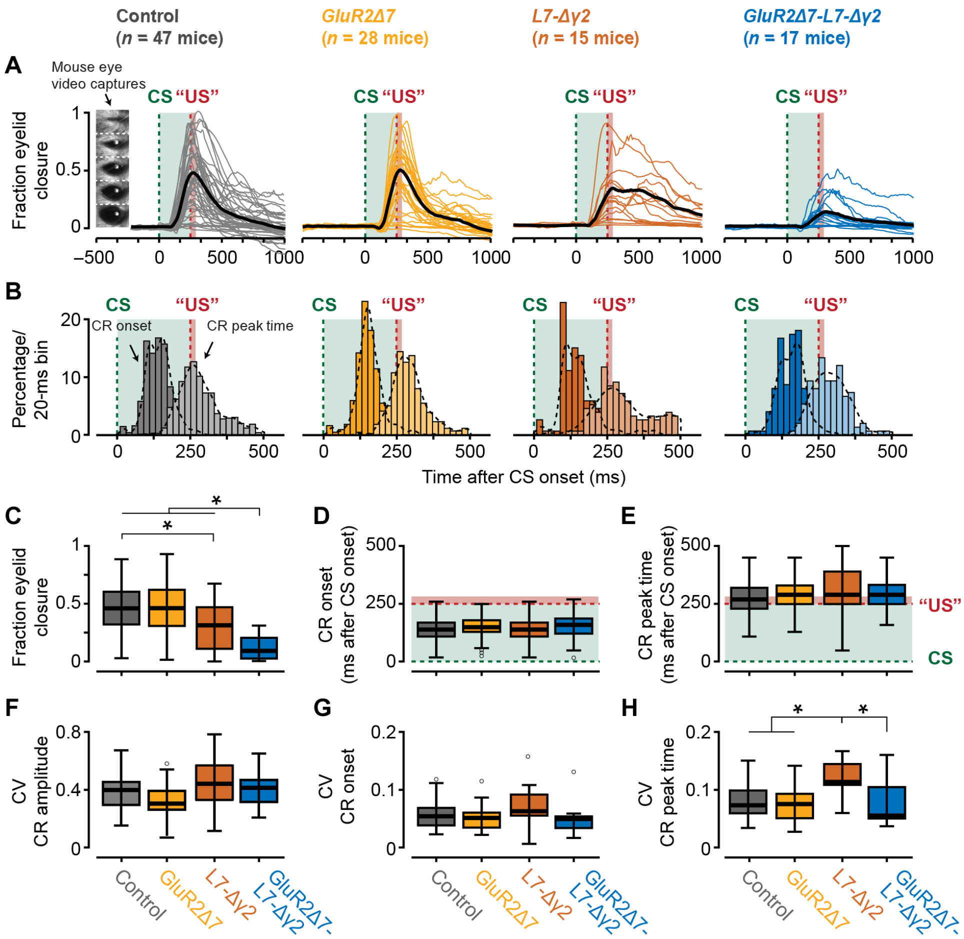

Fig. 3. Kinetic profile of eyeblink CRs during CS-only trials at the end of training. (**A**) Mouse individual average (colored) and total average (black) eyeblink traces of CS-only trials in the probe session following acquisition. Mouse eye video captures show eyelid closure ranging from 0 (fully open) to 1 (fully closed). *GluR2Δ7-L7-Δγ2* mice have significantly smaller FEC values than the other three groups. (**B**) Peristimulus histogram plots with a Gaussian kernel density estimate (black dashed line) showing the distribution of CR onset (dark filled bars) and CR peak time (light filled bars) relative to CS and US onset in paired CS-US trials for session 11 (probe). Green dashed lines indicate CS onset, and red dashed lines denote US onset; light green and light red fill indicate CS and US duration, respectively. (**C**) Mice carrying the *GluR2Δ7-L7-Δγ2* mutation have significantly lower FEC values than the three other groups. In addition, *L7-Δγ2* mice have significantly lower FEC values than control mice. FEC value is based on all CS-only trials in the probe session and represents the highest peak in the CS-US interval. (**D** and **E**) No significant difference was established for the average latency to CR onset and latency to CR peak. Both CR onset and CR peak time are based only on trials in which a CR was present (that is, FEC > 0.1 in the CS-US interval). Green dashed lines indicate CS onset, and red dashed lines denote US onset; light green and light red fill indicate CS and US duration, respectively. (**F** and **G**) No significant difference was established for CV values on CR amplitude and latency to CR onset. (**H**) As can be noted in the raw traces in (A), *L7-Δγ2* mice have a more jittery CR peak time, which results in a significantly higher CV value compared to the other three groups. In all panels, we refer to "CR" if only trials with an FEC > 0.1 are included and to "FEC" if all trials are included. For complete statistics, we refer to table S2; *$P < 0.05$.

DISCUSSION

Together, these data indicate that the strong phenotype in eyeblink conditioning in the *GluR2Δ7-L7-Δγ2* mice cannot be explained by the abnormal baseline firing patterns of their PCs. Instead, the most parsimonious explanation is that the simple spike suppression required for eyeblink conditioning is facilitated by both PF-PC LTD and MLI-PC FFI and that ablating only one of these mechanisms will elicit processes that can at least partly compensate for the deficit induced. It has been shown that deleting $GABA_A$ receptors from PCs, as occurs in the *L7-Δγ2* mice, will reduce the efficacy of the excitatory PF to PC synapse (*19*). These presumptively homeostatic mechanisms may well keep the excitatory-inhibitory inputs in balance and still permit simple spike suppression to be induced. This notion is further supported by the observation that combined PF and CF stimulation may lead to concurrent LTD of the PF-PC synapse and LTP of the PF-MLI synapse in vivo (*27*).

L7-Δγ2 mice have a stronger phenotype, in both their simple spike firing regularity (higher CV2) and CR peak time regularity (lower CV), than *GluR2Δ7-L7-Δγ2* mice. It is unknown whether more regular simple spikes and more jittered CR peak times are causally related, but this finding does suggest that, in addition to simple spike rate coding, simple spike temporal coding contains important functional features for cerebellar learning (*26*). It is interesting that the added PF-PC LTD impairment in the *GluR2Δ7-L7-Δγ2* mice seems to partially "rescue" simple spike and CR peak time regularity. In terms of simple spikes, the reduced attenuation of PF-PC input in this mutant could lead to a stronger displacement of simple spike timings due to stronger PF input, in absence of FFI. A plausible explanation

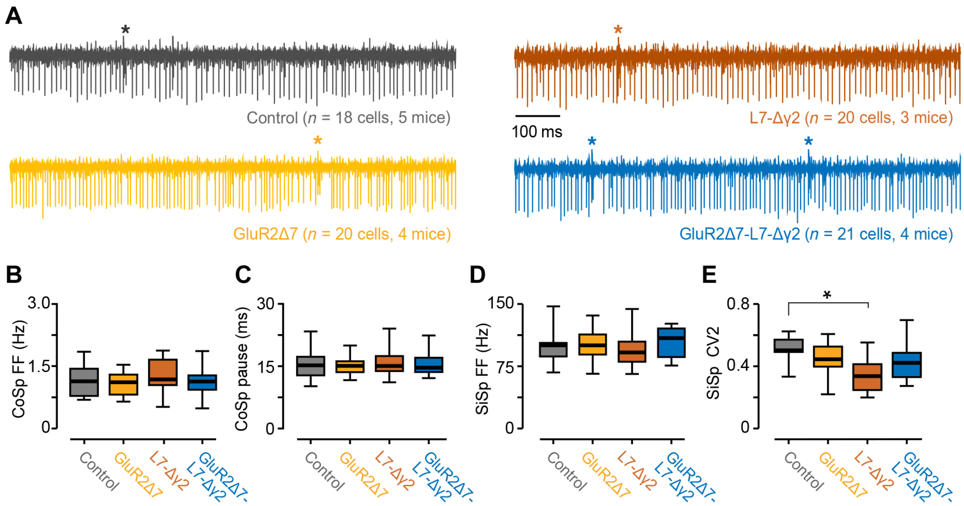

Fig. 4. *GluR2Δ7-L7-Δγ2* mice have no gross abnormalities in spontaneous firing behavior in vivo. (**A**) Raw examples of in vivo PC recordings from lobules I to V for all four groups. For (**B**) complex spike (CoSp) firing frequencies, (**C**) simple spike pauses following complex spikes, and (**D**) simple spike (SiSp) firing frequencies, no differences were found between controls and any of the mutant groups. (**E**) Unlike *L7-Δγ2* mice, *GluR2Δ7-L7-Δγ2* mice have no significantly higher simple spike regularity, as shown by the lower CV2 value. For complete statistics, we refer to table S3; $^*P < 0.05$.

for the lack of a CR timing phenotype in *GluR2Δ7-L7-Δγ2* mice could be the very low CR expression and the fact that a real timing deficit is more prominently present in movements with bigger amplitude. It should be noted that, in all analyses on CR timing, we corrected for FEC, since it is known that CRs that peak too early or too late typically have an amplitude or FEC value of less than 0.25 (fig. S2).

Whether induction of PF-PC LTD is completely blocked in the *GluR2Δ7-L7-Δγ2* mice under physiological circumstances is unclear. Recently, it was shown that some PF-PC LTD can still be induced in *GluR2Δ7* mice when the PF stimulus conditions are intensified; the CF stimulus is replaced by a strong somatic depolarization of the PC, and their stimulus interval is shortened (*28*). As pointed out by Hesslow *et al.* (*23*) and Titley and Hansel (*24*), many of the LTD-induction protocols have temporal characteristics that do not match those of eyeblink conditioning. Therefore, we have chosen to induce LTD with a protocol that closely mimics the temporal aspects of eyeblink conditioning, similar to what has been used previously by the Hansel group (*22*), using a more subtle PF stimulation followed by a single CF activation after a 110-ms delay. We find a significant behavioral phenotype that can be associated with an LTD blockage following the GluR2Δ7 genetic manipulation in conjunction with MLI blockage. Thus, even if LTD induction would only be partly impaired in the GluR2Δ7 mouse (depending on the induction protocol used), our behavioral data indicate that this difference in sensitivity for LTD induction is apparently still sufficient to allow for behavioral differences to occur.

Here, we used the PCP2-cre 2Mpin/J line, for which it has been reported that Cre may also be expressed by ±3% of the MLIs (*29*). Still, for our research on the *GluR2Δ7-L7-Δγ2* mutants, this line appeared suitable since we intended to block MLI-PC transmission and since the *GluR2Δ7-L7-Δγ2* mutants can be expected to have a 3% MLI Cre expression similar to that of the *L7-Δγ2* mutants, which served as controls. Thus, this potential caveat cannot explain the severe learning phenotype in the triple mutants.

Although eyeblink conditioning in *GluR2Δ7-L7-Δγ2* mice was severely affected, they do undeniably show some CRs at the end of the training. These eyeblink CRs are properly timed; that is, they peak around the onset of the expected US. Moreover, they do not show the higher CV for the latency to CR peak as found in the *L7-Δγ2* mutants (Fig. 3H), which probably occurred because of their relatively low expression level. Our findings in the *GluR2Δ7-L7-Δγ2* mice suggest additional neural mechanisms that contribute to PC simple spike suppression. It is unclear at this point whether PF-PC LTD and MLI-PC inhibition are indeed the only factors driving the PC simple spike suppression or only facilitate it by optimizing the PC's inputs that transmit the CS information. In line with recent findings supporting a more neurocentric instead of exclusively circuit-synaptocentric view on learning, such a mechanism might well involve a temporal memory that is partly formed *inside* the PC itself (*20*, *30*). Such a cell-intrinsic learning mechanism, however, may still depend on optimized synaptic inputs provided by PFs and MLIs. Our finding that only a concurrent disruption of PF-PC LTD and MLI-PC inhibition could severely impair eyeblink conditioning, but not completely block learning, rejects the idea that a single form of neural plasticity is essential and sufficient, and it supports the notion that synaptic and intrinsic plasticity synergistically contribute to form a temporal memory in the cerebellum (*25*).

MATERIALS AND METHODS

Subjects and generation of mice

For all experiments, we used male and female mice with a C57Bl/6 background (individually housed under 12-hour light/12-hour dark cycles with food ab libitum). For in vitro electrophysiology experiments, we used mice aged 5 to 20 weeks; for in vivo electrophysiology and eyeblink conditioning, mice were 15 to 25 weeks old. We made use of three different transgenic mouse lines. First, *GluR2Δ7* KI mice lack the last seven amino acids at the intracellular C-terminal tail, thereby disrupting the interaction of GluR2 with PICK1 and GRIP1/2, in turn disrupting the internalization of AMPA receptors, which impairs PF-PC LTD (*21*, *31*). Second, *L7-Δγ2* mice have a PC-specific (L7) ablation of the γ2 subunit of the $GABA_A$ receptors, resulting in impaired FFI provided by MLIs (*6*, *19*). For the L7-Δγ2 mice, we first generated *γ2I77lox* mice by flanking exon 4 of the *Gabrg2* gene with *loxP* sites and changing the codon encoding F77 in exons 4 to I, which resulted in a neutral amino acid substitution. Next, homozygous *γ2I77lox* were crossed with mice hemizygous for the PC-specific *L7-cre* transgene and heterozygous for *γ2I77lox* (*32*, *33*). For experiments, *L7-cre γ2I77lox/γ2I77lox* mice (L7-Δγ2) and *γ2I77lox/γ2I77lox* mice (controls) were used. Third, *GluR2Δ7-L7-Δγ2* mice, which lack both PF-PC LTD and MLI FFI, were generated by crossbreeding female mice hemizygous for *L7-cre* and homozygous for *γ2I77lox/γ2I77lox* with male homozygous GluR2Δ7 KI mice (= F_0). Next, F_1 female mice hemizygous for *L7-cre* and heterozygous for both *γ2I77lox/γ2I77lox* and *GluR2Δ7* were crossed with F_1 male mice heterozygous for both *γ2I77lox/γ2I77lox* and GluR2Δ7. This F_1 breeding generated F_2 mice, which were hemizygous for *L7-cre* and homozygous for both *γ2I77lox/γ2I77lox* and *GluR2Δ7*, and F_2 mice homozygous for both *γ2I77lox/γ2I77lox GluR2Δ7*. F_2 mice were used in experiments. F_2 mice homozygous for both *γ2I77lox/γ2I77lox* and *GluR2Δ7* were pooled with *GluR2Δ7* KI mice. As controls, we used pooled data from littermate *GluR2Δ7* s and *γ2I77lox/γ2I77lox* mice. All mice were genotyped by performing polymerase chain reaction analyses of genomic DNA at 2 to 3 weeks postnatal and once again postmortem. All experiments were approved by the Dutch Ethical Committee for animal experiments and were in accordance with the Institutional Animal Care and Use Committee (Erasmus MC).

In vitro electrophysiology

Decapitation and preparation

Following isoflurane anesthesia, mice were decapitated, and the cerebellum was obtained and put in an ice-cold "slicing medium" containing 3 mM *N*-methyl-D-glucamine, 93 mM HCl, 2.5 mM KCl, 1.2 mM $NaHPO_4$, 30 mM $NaHCO_3$, 25 mM glucose, 20 mM Hepes, 5 mM Na-ascorbate, 3 mM Na-pyruvate, 2 mM thiourea, 10 mM $MgSO_4$, 0.5 mM $CaCl_2$, and 5 mM *N*-acetyl-L-cysteine that was carbogenated continuously (95% O_2 and 5% CO_2). Sagittal slices (250 mm thick) of the cerebellar vermis were cut using a vibrotome (VT1200S, Leica) and put in carbogenated artificial cerebrospinal fluid (ACSF) containing 124 mM NaCl, 5 mM KCl, 1.25 mM Na_2HPO_4, 2 mM $MgSO_4$, 2 mM $CaCl_2$, 26 mM $NaHCO_3$, and 20 mM D-glucose, for at least 1 hour at 34° ± 1°C before the start of the experiment. All slice physiology was done at 34° ± 1°C in the presence of 100 mM picrotoxin except for the sIPSC recordings. Whole-cell patch-clamp recording was performed with an EPC9 amplifier (HEKA Electronics). Recordings were excluded if the series (Rs) or input resistances (Ri) changed by 20% during the experiment, which was determined using a hyperpolarizing voltage step relative to the −65-mV holding potential. For whole-cell recordings, PCs were visualized using an upright microscope (Axioskop 2 FS, Carl Zeiss) equipped with a 40× objective. Recording electrodes [3 to 5 megohms, outside diameter (OD), 1.65 mm; interior diameter (ID), 1.11 mm; World Precision Instruments] were filled with an intracellular solution containing 120 mM K-gluconate, 9 mM KCl, 10 mM KOH, 4 mM NaCl, 10 mM Hepes, 28.5 mM sucrose, 4 mM Na_2ATP, and 0.4 mM Na_3GTP (pH 7.25 to 7.35 with an osmolarity of 295 ± 5).

PF-PC transmission

For PF-PC transmission, we used various interstimulus intervals (50 to 200 ms). For CF stimulation, similar electrodes (filled with ACSF) were positioned near the patched PC soma in the surrounding granule layer.

Spontaneous inhibitory postsynaptic current

For the recording of sIPSCs, we used an intracellular solution containing 150 mM CsCl, 1.5 mM $MgCl_2$, 0.5 mM EGTA, 4 mM Na_2ATP, 0.4 mM Na_3GTP, 10 mM Hepes, and 5 mM QX314 (pH 7.25 to 7.35 with an osmolarity of 295 ± 5).

PF-PC LTD induction

For PF-PC LTD induction, we recorded from lobules V and VI. Recordings were done in voltage clamp, except for the tetanus, which consisted of 100-Hz PF stimulation in eight pulses followed by a 110-ms delay of single CF activation at 1 Hz for 5 min. We evaluated the synaptic plasticity by the change in PF-EPSC (baseline at 0.05 Hz) relative to the mean value calculated during the 5-min-long baseline pre-tetanus (*22*).

Data analysis

Data analysis was performed using Clampfit software (Molecular Devices).

Eyeblink conditioning

Surgery

Mice were anesthetized with an isoflurane/oxygen mixture (5% for induction, 1.5 to 2% for maintenance), and body temperature was kept constant at 37°C. Eyes were protected against drying using an eye lubricant (Duratears). After a local scalp injection of bupivacaine hydrochloride (2.5 mg/ml, Bupivacaine Actavis), we made a sagittal scalp incision of 2 to 3 cm length. Next, we carefully removed the exposed periosteum and roughened the surface of the skull using an etchant gel (Kerr). After this, a small messing block (10 mm × 4 mm × 3 mm) with one screw thread and two additional pinholes was placed on the skull using OptiBond primer and adhesive (Kerr) and Charisma (Heraeus Kulzer). The surgical placement of this so-called pedestal allowed for head fixation during the eyeblink conditioning experiments.

Behavioral training

All behavioral experiments were conducted using head-fixed mice that were placed on top of a cylindrical treadmill on which they were allowed to walk freely (Fig. 1A). The treadmill consisted of a foam roller (diameter, ±15 cm; width, ±12 cm; Exervo, TeraNova EVA) with a horizontal metal rod through the axis that was connected with a ball bearing construction to two solid vertical metal poles. A horizontal messing bar was fixated to the same vertical poles at 3 to 5 cm above the treadmill. Mice were head-fixed to this bar using one screw and two pins, thereby ensuring perfect head fixation [for further details, see (*34*)]. National Instruments (NI-PXI) equipment was used to control experimental parameters and to acquire the eyelid position signal. Eyelid movements were recorded with the MDMT, which makes use of an NVE giant magnetoresistance magnetometer, positioned above the left upper eyelid, that measures movements of a minuscule magnet (1.5 mm × 0.7 mm × 0.5 mm) that is placed on the left lower eyelid of the animal with superglue (cyanoacrylate). This way, MDMT allows high spatiotemporal detection of eyelid kinematics [for further details, see (*35*)]. The CS was a green LED light (CS duration, 280 ms; LED diameter, 5 mm) placed 10 cm in front of the mouse's head. Because we performed our experiments in almost complete darkness, this small LED light was a salient stimulus, which could be easily detected by both eyes. The US consisted of a weak air puff applied to the eye (30 psi; duration, 30 ms), which was controlled by an API MPPI-3 pressure injector, and delivered via a 27.5-gauge needle that was perpendicularly positioned at 0.5 to 1 cm from the center of the left cornea. The training consisted of 3 daily habituation sessions, 1 baseline measurement, 5 or 10 daily acquisition sessions, and 1 probe session immediately after the last training session. During the habituation sessions, mice were placed in the setup for 30 to 45 min, during which the air puff needle (for US delivery) and green LED (for CS delivery) were positioned properly but no stimuli were presented. On the day of acquisition session 1, each animal first received 20 CS-only trials as a baseline measure, to establish that the CS did not elicit any reflexive eyelid closure. During each daily acquisition session, the animals received either 100 or 200 paired CS-US trials, separated over 10 or 5 daily acquisition sessions, respectively. The interval between the onset of CS and that of US was set at 250 ms. Because of an inherent 14-ms delay in the delivery of the air puff, we triggered the air puff at 236 ms after CS onset so that it would hit the cornea exactly at 250 ms after CS onset. The intertrial interval was set according to the following constraints: At least 10 s had to elapse, the eyelid had to be open below a predetermined threshold of 50% of a full eyelid closure, and eyelid position had to be stable for at least 2 s for a trial to begin. Immediately after acquisition session 10, we started a probe session, during which we presented another 100 paired CS-US trials, but now intermingled with 30 CS-only trials. During all training sessions, the experimenter carefully inspected threshold and stability parameters and adjusted them if necessary. All experiments were performed at approximately the same time of day by the same experimenter.

Data analysis

Individual eyeblink traces were analyzed automatically with custom computer software (LabVIEW or MATLAB). First, 2000-ms eyeblink traces were imported and filtered in forward and reverse directions with a low-pass Butterworth filter using a cutoff frequency at 50 Hz. Second, trials with significant activity in the 500-ms pre-CS period (>7 * interquartile range) were regarded as invalid for further analysis. Third, trials were normalized by aligning the 500-ms pre-CS baselines and calibrating the signal so that the size of a full blink was 1 (FEC). Fourth, in valid normalized trials, all eyelid movements larger than 0.1 and with a latency to CR onset between 50 and 250 ms and a latency to CR peak of 100 to 250 ms (both relative to CS onset) were considered as CRs. For CS-only trials in the probe session, we used the exact same criteria except that the latency to CR peak time was set at 100 to 500 ms after CS onset. Additionally, we determined for each individual trial the following parameters: (i) maximum eyelid closure (= FEC) in the CS-US interval, (ii) CR amplitude, (iii) latency to CR onset, (iv) latency to CR peak, (v) latency to UR onset, and (vi) latency to first UR peak. For (i), we used all valid trials; for (ii) to (iv), we only used the trials in which a CR was present; for (v) and (vi), we used US-only trials in the baseline session. Fifth, on the basis of this trial-by-trial analysis, we calculated for each session per mouse the percentage of eyeblink CRs and the mean median, SD, and CV of all other outcome measures. Sixth, statistical effects of session and genotype on all outcome measures were established in R version 1.1.442 using linear mixed-effect models (LMMs). All our outcome measures except for CR peak time included group, session number (categorical), and their interaction as fixed effects. The random effect included mouse. (R syntax: *lme (measure) ~ group + session + session:group), data = all_data, random = list (mouse = pdDiag (form = ~ poly (session, 2))), method = "REML", na.action = na.exclude)).* For CR peak time, we used a modified model, adding FEC as a fixed effect, since it is known that smaller CRs at the beginning of training have worse timing compared to CRs at the end of training (Fig. 2C and fig. S2). (R syntax: *lme (CRpeaktime) ~ group + session + session:group + FEC), data = all_data, random = list (mouse = pdDiag (form = ~ poly (session,2))), method = "REML", na.action = na.exclude)).* Data were considered statistically significant if $P < 0.05$, and we used false discovery rate correction for multiple comparisons.

In vivo PC recordings

Surgery

Mice were surgically prepared following the same procedure as described for eyeblink conditioning. Additionally, a craniotomy (diameter, 2 to 3 mm) was performed on the occipital bone to perform extracellular PC recordings from both the anterior and posterior cerebellum. A small rim of Charisma was made around the craniotomy, and anti-inflammatory (dexamethasone, 4 mg/ml) solution was applied inside, after which the chamber was closed with a very low viscosity silicone elastomer sealant (Kwik-Cast, World Precision Instruments). After surgery, mice had 5 days to recover.

Recordings

Extracellular PC recordings were conducted using head-fixed mice that were placed on top of a cylindrical treadmill system as described above. Mice were first habituated for 3 days to the treadmill. PCs were recorded from vermal lobules I to V and lobules VI to X using glass micropipettes (OD, 2.0 mm; ID, 1.16 mm; tip, 2 to 5 μm, impedance, 2 to 5 milliohms; Harvard Apparatus). Single-unit PCs were recorded for 2 to 5 min. Single-unit recording was identified online by the presence of a short simple spike pause (20 to 50 ms) after each complex spike. To verify recording locations, we made small alcian blue injections after recording sessions.

Analysis

In vivo recordings were analyzed offline using custom scripts in MATLAB (Mathworks) and SPSS 24. Average simple spike and complex spike firing were calculated. Simple spike firing regularity was investigated using the CV2 value, which was calculated as $2 * |\mathrm{ISI}_{n+1} - \mathrm{ISI}_n| / (\mathrm{ISI}_{n+1} - \mathrm{ISI}_n)$.

SUPPLEMENTARY MATERIALS

Supplementary material for this article is available at http://advances.sciencemag.org/cgi/content/full/4/10/eaas9426/DC1

Fig. S1. Analysis explanation of raw eyeblink traces.

Fig. S2. Correlation between eyeblink amplitude and eyeblink peak time in paired CS-US trials in sessions 1 to 10.

Fig. S3. Performance of reflexive eyelid closures (UR) was similar between groups.

Table S1. In vitro electrophysiology: LTD induction, sIPSC, and paired-pulse facilitation.

Table S2. Pavlovian eyeblink conditioning.

Table S3. In vivo single-unit PC recordings from anterior cerebellar cortex.

REFERENCES AND NOTES

1. H. J. Boele, M. M. Ten Brinke, C. I. De Zeeuw, Classical conditioning of timed motor responses: Neural coding in cerebellar cortex and cerebellar nuclei, in *The Neural Codes of the Cerebellum*, D. H. Heck, Ed. (Academic Press, 2015), pp. 53–96.
2. J. H. Freeman, A. B. Steinmetz, Neural circuitry and plasticity mechanisms underlying delay eyeblink conditioning. *Learn. Mem.* **18**, 666–677 (2011).
3. G. Hesslow, Correspondence between climbing fibre input and motor output in eyeblink-related areas in cat cerebellar cortex. *J. Physiol.* **476**, 229–244 (1994).
4. A. Mostofi, T. Holtzman, A. S. Grout, C. H. Yeo, S. A. Edgley, Electrophysiological localization of eyeblink-related microzones in rabbit cerebellar cortex. *J. Neurosci.* **30**, 8920–8934 (2010).
5. S. A. Heiney, J. Kim, G. J. Augustine, J. F. Medina, Precise control of movement kinematics by optogenetic inhibition of Purkinje cell activity. *J. Neurosci.* **34**, 2321–2330 (2014).
6. M. M. ten Brinke, H.-J. Boele, J. K. Spanke, J.-W. Potters, K. Kornysheva, P. Wulff, A. C. H. G. IJpelaar, S. K. E. Koekkoek, C. I. De Zeeuw, Evolving models of Pavlovian conditioning: Cerebellar cortical dynamics in awake behaving mice. *Cell Rep.* **13**, 1977–1988 (2015).
7. M. Thurling, F. Kahl, S. Maderwald, R. M. Stefanescu, M. Schlamann, H.-J. Boele, C. I. De Zeeuw, J. Diedrichsen, M. E. Ladd, S. K. E. Koekkoek, D. Timmann, Cerebellar cortex and cerebellar nuclei are concomitantly activated during eyeblink conditioning: A 7T fMRI study in humans. *J. Neurosci.* **35**, 1228–1239 (2015).

8. A. B. Steinmetz, J. H. Freeman, Localization of the cerebellar cortical zone mediating acquisition of eyeblink conditioning in rats. *Neurobiol. Learn. Mem.* **114**, 148–154 (2014).
9. D.-A. Jirenhed, F. Bengtsson, G. Hesslow, Acquisition, extinction, and reacquisition of a cerebellar cortical memory trace. *J. Neurosci.* **27**, 2493–2502 (2007).
10. H. E. Halverson, A. Khilkevich, M. D. Mauk, Relating cerebellar Purkinje cell activity to the timing and amplitude of conditioned eyelid responses. *J. Neurosci.* **35**, 7813–7832 (2015).
11. C. Hansel, D. J. Linden, E. D'Angelo, Beyond parallel fiber LTD: The diversity of synaptic and non-synaptic plasticity in the cerebellum. *Nat. Neurosci.* **4**, 467–475 (2001).
12. M. D. Mauk, D. V. Buonomano, The neural basis of temporal processing. *Annu. Rev. Neurosci.* **27**, 307–340 (2004).
13. N. L. Cerminara, J. A. Rawson, Evidence that climbing fibers control an intrinsic spike generator in cerebellar Purkinje cells. *J. Neurosci.* **24**, 4510–4517 (2004).
14. H. Zhou, Z. Lin, K. Voges, C. Ju, Z. Gao, L. W. J. Bosman, T. J. H. Ruigrok, F. E. Hoebeek, C. I. De Zeeuw, M. Schonewille, Cerebellar modules operate at different frequencies. *eLife* **3**, e02536 (2014).
15. E. Galliano, Z. Gao, M. Schonewille, B. Todorov, E. Simons, A. S. Pop, E. D'Angelo, A. M. J. M. van den Maagdenberg, F. E. Hoebeek, C. I. De Zeeuw, Silencing the majority of cerebellar granule cells uncovers their essential role in motor learning and consolidation. *Cell Rep.* **3**, 1239–1251 (2013).
16. J. P. Welsh, H. Yamaguchi, X.-H. Zeng, M. Kojo, Y. Nakada, A. Takagi, M. Sugimori, R. R. Llinás, Normal motor learning during pharmacological prevention of Purkinje cell long-term depression. *Proc. Natl. Acad. Sci. U.S.A.* **102**, 17166–17171 (2005).
17. M. Schonewille, Z. Gao, H. J. Boele, M. F. V. Veloz, W. E. Amerika, A. A. Simek, M. T. De Jeu, J. P. Steinberg, K. Takamiya, F. E. Hoebeek, D. J. Linden, R. L. Huganir, C. I. De Zeeuw, Reevaluating the role of LTD in cerebellar motor learning. *Neuron* **70**, 43–50 (2011).
18. W. Mittmann, U. Koch, M. Häusser, Feed-forward inhibition shapes the spike output of cerebellar Purkinje cells. *J. Physiol.* **563**, 369–378 (2005).
19. P. Wulff, M. Schonewille, M. Renzi, L. Viltono, M. Sassoè-Pognetto, A. Badura, Z. Gao, F. E. Hoebeek, S. van Dorp, W. Wisden, M. Farrant, C. I. De Zeeuw, Synaptic inhibition of Purkinje cells mediates consolidation of vestibulo-cerebellar motor learning. *Nat. Neurosci.* **12**, 1042–1049 (2009).
20. F. Johansson, D.-A. Jirenhed, A. Rasmussen, R. Zucca, G. Hesslow, Memory trace and timing mechanism localized to cerebellar Purkinje cells. *Proc. Natl. Acad. Sci. U.S.A.* **111**, 14930–14934 (2014).
21. J. P. Steinberg, K. Takamiya, Y. Shen, J. Xia, M. E. Rubio, S. Yu, W. Jin, G. M. Thomas, D. J. Linden, R. L. Huganir, Targeted in vivo mutations of the AMPA receptor subunit GluR2 and its interacting protein PICK1 eliminate cerebellar long-term depression. *Neuron* **49**, 845–860 (2006).
22. C. Piochon, A. D. Kloth, G. Grasselli, H. K. Titley, H. Nakayama, K. Hashimoto, V. Wan, D. H. Simmons, T. Eissa, J. Nakatani, A. Cherskov, T. Miyazaki, M. Watanabe, T. Takumi, M. Kano, S. S.-H. Wang, C. Hansel, Cerebellar plasticity and motor learning deficits in a copy-number variation mouse model of autism. *Nat. Commun.* **5**, 5586 (2014).
23. G. Hesslow, D.-A. Jirenhed, A. Rasmussen, F. Johansson, Classical conditioning of motor responses: What is the learning mechanism? *Neural Netw.* **47**, 81–87 (2013).
24. H. K. Titley, C. Hansel, Asymmetries in cerebellar plasticity and motor learning. *Cerebellum* **15**, 87–92 (2015).
25. Z. Gao, B. J. van Beugen, C. I. De Zeeuw, Distributed synergistic plasticity and cerebellar learning. *Nat. Rev. Neurosci.* **13**, 619–635 (2012).
26. C. I. De Zeeuw, F. E. Hoebeek, L. W. J. Bosman, M. Schonewille, L. Witter, S. K. Koekkoek, Spatiotemporal firing patterns in the cerebellum. *Nat. Rev. Neurosci.* **12**, 327–344 (2011).
27. D.-A. Jirenhed, F. Bengtsson, H. Jörntell, Parallel fiber and climbing fiber responses in rat cerebellar cortical neurons in vivo. *Front. Syst. Neurosci.* **7**, 16 (2013).
28. K. Yamaguchi, S. Itohara, M. Ito, Reassessment of long-term depression in cerebellar Purkinje cells in mice carrying mutated GluA2 C terminus. *Proc. Natl. Acad. Sci. U.S.A.* **113**, 10192–10197 (2016).
29. L. Witter, S. Rudolph, R. T. Pressler, S. I. Lahlaf, W. G. Regehr, Purkinje cell collaterals enable output signals from the cerebellar cortex to feed back to Purkinje cells and interneurons. *Neuron* **91**, 312–319 (2016).
30. C. R. Gallistel, The coding question. *Trends Cogn. Sci.* **21**, 498–508 (2017).
31. J. Xia, H. J. Chung, C. Wihler, R. L. Huganir, D. J. Linden, Cerebellar long-term depression requires PKC-regulated interactions between GluR2/3 and PDZ domain–containing proteins. *Neuron* **28**, 499–510 (2000).
32. J. J. Barski, K. Dethleffsen, M. Meyer, Cre recombinase expression in cerebellar Purkinje cells. *Genesis* **28**, 93–98 (2000).
33. J. Oberdick, R. J. Smeyne, J. R. Mann, S. Zackson, J. I. Morgan, A promoter that drives transgene expression in cerebellar Purkinje and retinal bipolar neurons. *Science* **248**, 223–226 (1990).
34. S. N. Chettih, S. D. McDougle, L. I. Ruffolo, J. F. Medina, Adaptive timing of motor output in the mouse: The role of movement oscillations in eyelid conditioning. *Front. Integr. Neurosci.* **5**, 72 (2011).
35. S. K. E. Koekkoek, W. L. Den Ouden, G. Perry, S. M. Highstein, C. I. De Zeeuw, Monitoring kinetic and frequency-domain properties of eyelid responses in mice With magnetic distance measurement technique. *J. Neurophysiol.* **88**, 2124–2133 (2002).

Acknowledgments: We thank P. Bacilio and S. Dijkhuizen for their technical assistance on eyeblink conditioning experiments. **Funding:** This work was financially supported by the Netherlands Organization for Health Research and Development (ZonMw) (H.J.B. and C.I.D.Z.), Life Sciences (NWO-ALW) (C.I.D.Z.), European Research Council (ERC)–Advanced and ERC–Proof of Concept of the European Community (C.I.D.Z.), and the Erasmus MC Fellowship (H.J.B.). **Author contributions:** C.I.D.Z. and H.J.B. designed experiments. S.P. performed in vitro electrophysiology. L.V., M.M.T.B., and H.J.B. performed in vivo electrophysiology. A.C.H.I., H.J.B., and S.K.E.K. performed eyeblink conditioning. H.J.B., S.P., M.M.T.B., Z.G., and D.R. analyzed the data. H.J.B., M.M.T.B., S.P., and C.I.D.Z. wrote the manuscript. **Competing interests:** The authors declare that they have no competing interests. **Data and materials availability:** All data needed to evaluate the conclusions in the paper are present in the paper and/or the Supplementary Materials. Additional data related to this paper may be requested from the authors.

Submitted 8 January 2018
Accepted 23 August 2018
Published 3 October 2018
10.1126/sciadv.aas9426

Citation: H.-J. Boele, S. Peter, M. M. Ten Brinke, L. Verdonschot, A. C. H. IJpelaar, D. Rizopoulos, Z. Gao, S. K. E. Koekkoek, C. I. De Zeeuw, Impact of parallel fiber to Purkinje cell long-term depression is unmasked in absence of inhibitory input. *Sci. Adv.* **4**, eaas9426 (2018).